ELSEVIER

Nuclear Instruments and Methods in Physics Research B 181 (2001) 315–319

NIM B
Beam Interactions with Materials & Atoms

www.elsevier.com/locate/nimb

Diffusion-time-resolved ion-beam-induced charge collection from stripe-like test junctions induced by heavy-ion microbeams

B.N. Guo [a], M. El Bouanani [a], S.N. Renfrow [b], M. Nigam [a], D.S. Walsh [b], B.L. Doyle [b], J.L. Duggan [a], F.D. McDaniel [a,*]

[a] *Ion Beam Modification and Analysis Laboratory, Department of Physics, University of North Texas, P.O. Box 311427, Denton, TX 76203, USA*

[b] *Ion Beam Materials Research Laboratory, Sandia National Laboratories, MS 1056, P.O. Box 5800, Albuquerque, NM 87185, USA*

Abstract

To design more radiation-tolerant integrated circuits (ICs), it is necessary to design and test accurate models of ionizing-radiation-induced charge collection dynamics. A new technique, diffusion-time-resolved ion-beam-induced charge collection (DTRIBICC), is used to measure the average arrival time of the diffused charge, which is related to the average time of the arrival carrier density at the junction. Specially designed stripe-like test junctions are studied using a 12 MeV carbon microbeam with a spot size of ~1 μm. The relative arrival time of ion-generated charge and the collected charge are measured using a multiple parameter data acquisition system. A 2-D device simulation code, MEDICI, is used to calculate the charge collection dynamics on the stripe-like test junctions. The simulations compare well with experimental microbeam measurements. The results show the importance of the diffused charge collection by junctions, which is especially significant for single-event upsets (SEUs) and multiple-event upsets (MEUs) in electronic devices. The charge sharing results also indicate that stripe-like junctions may be used as position-sensitive detectors with a resolution of ~0.1 μm.

PACS: 61.82.F; 07.78; 85.30.K

Keywords: Heavy-ion microprobe; Single-event upset; Diffusive charge collection; Average arrival time; Diffusion-time-resolved ion-beam-induced charge collection

1. Introduction

Since the charge signals defining data states are reduced by voltage and area scaling, integrated circuits (ICs) have a higher susceptibility to ionizing-radiation-induced effects [1]. To design more radiation-tolerant ICs, ion microbeam techniques have been used, such as single-event upset (SEU) imaging and ion-beam-induced charge collection (IBICC) [2–4]. To evaluate the response of microcircuits immediately following ion strikes, time-resolved IBICC (TRIBICC) has been developed at Sandia National Laboratory [5]. In this paper, a

* Corresponding author. Tel.: +1-940-565-3251; fax: +1-940-565-2227.

E-mail address: mcdaniel@unt.edu (F.D. McDaniel).

0168-583X/01/$ - see front matter
PII: S0168-583X(01)00488-8

new technique, diffusion-time-resolved IBICC (DTRIBICC), is proposed to measure the average arrival time of charge collection [6].

As IC design moves to a smaller scale, models based on the diffusion mechanism can interpret some experimental results better than those based on the drift- and funneling-assisted mechanisms [7]. The time duration of charge collection by the charge collection node can be estimated to account for the diffused charge collection [8].

Model simulation results are obtained using the 2-D MEDICI code [9]. Based on a drift–diffusion model, MEDICI can be used to study steady-state or time-dependent injection of electrons and holes. Electron–hole pair generation, based on SRIM calculations along the ion track, is incorporated to simulate the induced charge transportation in the devices [10].

2. Experimental and simulation details

The Sandia microprobe was utilized to produce a 12 MeV carbon beam with ~1 μm beam spot size. The cross-section of the stripe junctions is shown in Fig. 1. The outer and inner diodes are separately connected to external package wiring. P and As are used to form n+, and the B-doped p-substrate has a p+ retrograde B well. The junction doping profiles were incorporated into the MEDICI simulations. The simulations include carrier–carrier scattering and field-dependent mobility, concentration-dependent recombination, and bandgap narrowing [9].

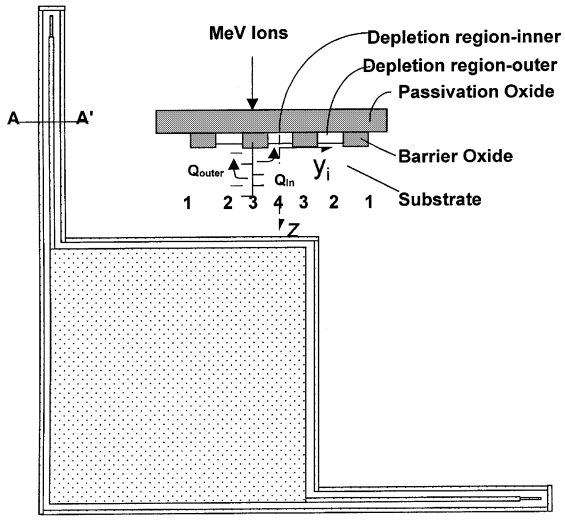

Fig. 1. Cross-sectional view of stripe-like junctions for the DTRIBICC measurements, which are a part of an outer–inner diode test structure. The 2-μm wide stripes are separated by 2-μm wide oxide barriers to approximate node to node spacing in memories.

The relative arrival time (diffusion time) was measured between the outer–inner diode test structure using the DTRIBICC technique. Two separated 4 V reverse biases were applied to the outer and inner diodes through two preamplifiers. The p-substrate was grounded. The timing outputs from the two preamplifiers were fed into two constant fraction discriminators (CFD). The fast timing outputs from the CFDs were then fed into a TAC as the start (from outer junction) and stop (from inner junction) signals. The TAC signals were coincidentally recorded along with striking spot coordinates and collected charge from the outer and inner junctions. The TAC range was set at 100 ns. A 48 ns offset was inserted into the stop signal channel. The time scale was calibrated with a nanosecond delay box. The total charge collected by a pin diode was used to calibrate the charge collection electronics. The counting rate of charge collection was about 400 counts/s. The microbeam was scanned over a 60 μm × 60 μm area.

It is assumed that the charge is collected by the junction centers. Referring to Fig. 1, if the ion strikes at a distance y_i from the center of the inner junction, and penetrates a distance z into the sample, it is straightforward to show that this arrival time difference, Δt, is just

$$\Delta t = \frac{(d - |y_i|)^2 + z^2}{D} - \frac{|y_i|^2 + z^2}{D} = \frac{d(d - 2|y_i|)}{D}, \tag{1}$$

where d is the junction centers separation (4 μm) and D is the diffusivity of electrons in Si. It is interesting that Δt is not a function of z, and therefore the charge that diffuses from any point along the trajectory of the ion will diffuse to these diodes with the same time.

3. Results and discussion

Figs. 2–4 are DTRIBICC charge collection measurements on the outer–inner junction test structure using a 12 MeV carbon microbeam. Figs. 2(a) and (b) are the cross-sectional views of the median filtered charge collected for the inner and outer junctions for $10 < x < 15$ μm, respectively. Fig. 3(a) plots the relative arrival time projection at the same slice view position. Fig. 3(b) is the histogram of the relative arrival time measurements. For all data presented here, the 48 ns delay is not subtracted from the experimental data. In Fig. 4, the collected charge by the outer junction is plotted against the collected charge by the inner junction. In Figs. 2–4, the numerical coding #1–4 corresponds to the striking positions defined in Fig. 1.

In Figs. 2 and 3(a), MEDICI simulation results are plotted for comparison. Based on MEDICI simulations, the transient currents versus time are obtained for the outer and inner junctions. Due to the symmetry of the junction, only half of the test structure is simulated.

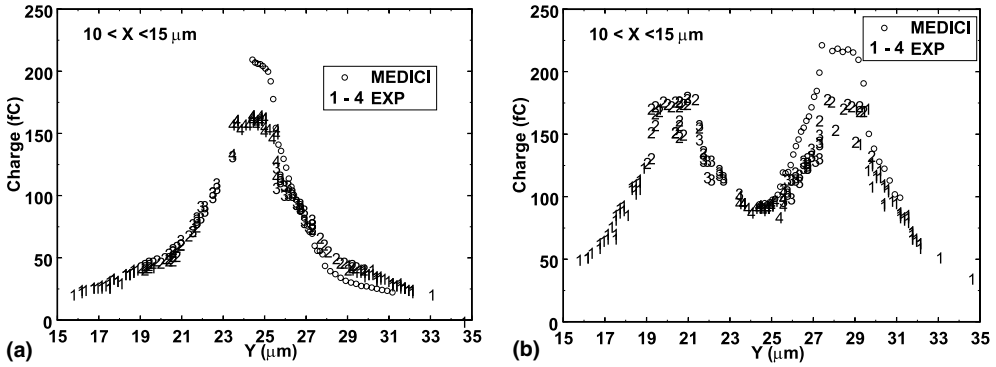

Fig. 2. Expanded cross-sectional view of charge collection by inner (a) and outer (b) junctions. MEDICI simulation results are also plotted for comparison. The numerical coding #1–4 corresponds to the positions shown in Fig. 1.

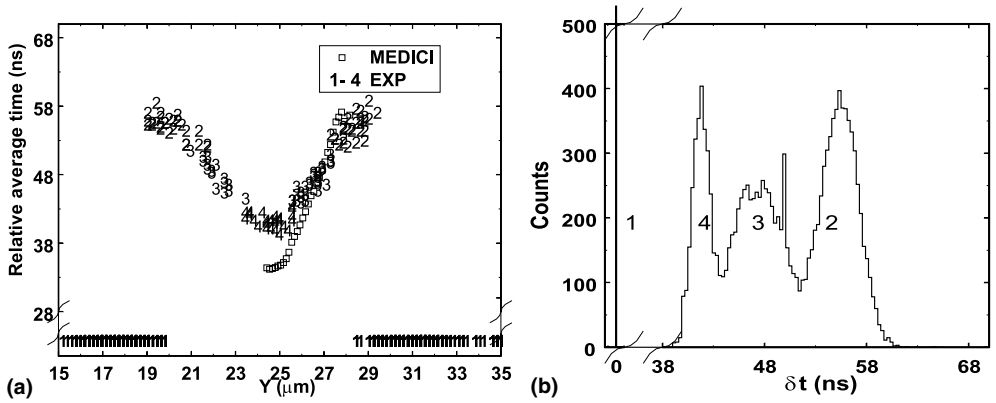

Fig. 3. DTRIBICC relative arrival time measurements on the outer–inner diodes. (a) is the expanded cross-sectional view of the relative arrival time (MEDICI simulation included), which also corresponds to positions of slice views in Fig. 2. (b) is the histogram of the relative arrival time measurements. The TAC start and stop signals were triggered by the timing outputs of two preamplifiers, connected to the outer and inner junctions, respectively. The start signals were delayed by 48 ns to increase the measurement dynamic scale. The four peaks $t = 0$, 52–63, 44–52, 35–44 ns are linked to the striking positions (#1–4) shown in Fig. 1. The $t = 0$ peak is out of scale.

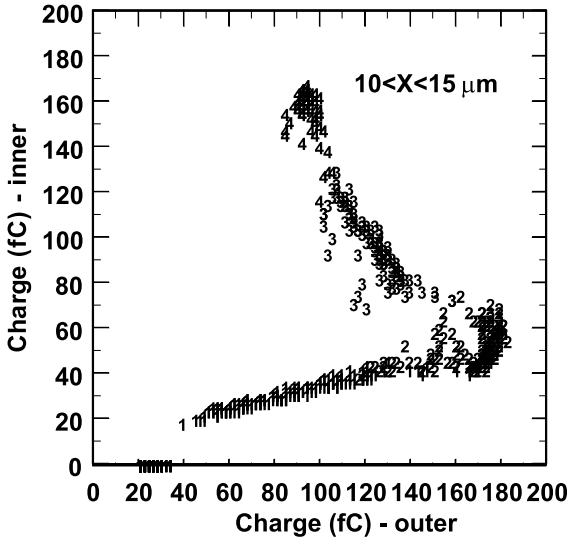

Fig. 4. Charge collection from the outer junction is plotted against that from the inner junction. The numerical coding corresponds to positions defined in Fig. 1.

The projections of charge collection and relative arrival time in Figs. 2 and 3(a) indicate that when ions strike outside of and far away from the outer junction, the charge is collected by the outer junction through the diffusion process and no charge is collected by the inner junction. As the beam strikes closer to the outer junction, the inner junction begins to pick up some charge through diffusion. As indicated in Fig. 4, the low threshold value of the CFD in the stop channel (inner junction) was about 40 fC or the minimum value of #2. If the charge collection by the inner junction is not enough to trigger the CFD, then the TAC resets itself and gives zero output as shown in Fig. 3(b) ($t = 0$ ns peak). Once the stop timing signals begin to be triggered, non-zero TAC signals are registered which correspond to the peak at 52–63 ns shown in Fig. 3(b). When the ions strike between the outer and inner junctions (peak at 44–52 ns in Fig. 3(b)), the induced charge is shared between the two junctions and the relative arrival time should follow Eq. (1). When ions strike in the middle of the outer and inner junctions (i.e. $|y_i| = d/2$ in Eq. (1)), the TAC will record the relative arrival time as 48 ns which corresponds to $\Delta t = 0$ in Eq. (1). If the data in Fig. 3(a) is fit to the straight line(s) derived in Eq. (1), the diffusivity, D, of electrons in Si is determined to be 18.5 cm^2/s, which corresponds to an electron mobility of 714 cm^2/V s. As ions directly strike the inner junction (peak at 38–44 ns in Fig. 3(b)), the outer junction will pick up some charge through diffusion.

Fig. 4 clearly reveals the charge sharing between the inner and outer junctions and also indicates the ion striking spots. Since the distance between the outer and inner junctions is only 2 μm, the position can be inferred based on the charge sharing with a potential ~0.1 μm resolution. Therefore, DTRIBICC forms the basis for a new type of position-sensitive detector for MeV ions with a resolution approaching 0.1 μm. This resolution could clearly be improved by optimizing the design of the diode stripe structure.

As shown in Figs. 2 and 3(a), it is clear that the charge collection and the relative arrival time predicted by the MEDICI simulations are in agreement with the experimental results. We believe the difference between the experimental and simulation results are due to limitations of the MEDICI code [9]. To better predict and compare with experimental results, 3D codes such as DAVINCI should be utilized to simulate correct ion track and test structure [11].

Since the experimental results were recorded in list mode, an off-line analysis of the collected data shows that ion-induced damage did not affect the charge collected by the junctions at the accumulated dose ~10 ions/μm^2. The relative arrival times were measured using two CFDs, which were triggered by the rising edges of the preamplifier signals. The timing uncertainty was affected by the uncertainty of the CFD and the capacitance of the junctions and was estimated to be about 0.5 ns.

4. Conclusions

The experimental results show the importance of diffused charge and charge sharing between adjacent junctions, which can result in MEUs. DTRIBICC, using relative arrival timing, represents an important new single-ion radiation effects microscopy for studying charge sharing. With a suitable start signal (e.g. secondary electrons from

the sample surface), the absolute average arrival time can be directly measured which can also be used to calibrate device design tools. Therefore, carrier transport properties such as minority carrier mobility can be directly measured. DTRI-BICC, on stripe-like junctions, may also be the basis for a new type of position-sensitive detector for MeV ions with a resolution of $\sim$0.1 μm.

Since very little charge was collected on the inner diode when ions struck outside the outer diodes, sensitive junctions could be shielded from distant ion strikes by using a perimeter-type diode structure. Such a perimeter shield could potentially ameliorate MEU effects. Similar structures could be used to optimize the engineering of layers to reduce SEUs in ICs.

Acknowledgements

Work supported in part by the NSF, the State of Texas – Advanced Technology Program, and the Robert A. Welch Foundation. Sandia is a multiprogram laboratory operated by Sandia Corporation, a Lockheed Martin Company for the US DoE under contract DE-AC04-94AL85000. The authors would like to thank T.J. Aton, E.B. Smith and R.C. Baumann of Texas Instruments Inc. for assistance with samples and for many helpful discussions.

References

[1] T.C. May, M.H. Woods, IEEE Trans. Electron Devices ED 26 (1979) 2.
[2] B.L. Doyle, K.M. Horn, D.S. Walsh, F.W. Sexton, Nucl. Instr. and Meth. B 64 (1992) 313.
[3] M.B.H. Breese, P.J.C. King, G.W. Grime, F. Watt, J. Appl. Phys. 72 (1992) 2097.
[4] K.M. Horn, B.L. Doyle, F.W. Sexton, J.S. Laird, A. Saint, M. Cholewa, G.J.F. Legge, Nucl. Instr. and Meth. B 77 (1993) 355.
[5] H. Schöne, D.S. Walsh, F.W. Sexton, B.L. Doyle, P.E. Dodd, J.F. Aurand, R.S. Flores, N. Wing, Nucl. Instr. and Meth. B 158 (1999) 424.
[6] B.N. Guo, Ph.D. dissertation, University of North Texas, 2000.
[7] L.D. Edmonds, IEEE Trans. Nucl. Sci. NS 38 (1996) 3207.
[8] L.D. Edmonds, IEEE Trans. Nucl. Sci. NS 43 (1996) 2347.
[9] DAVINCI/MEDICI device simulation tools, Avant! Corporation, 46871 Bayside Parkway, Fremont, CA 94538, http://www.avanticorp.com/.
[10] J.F. Ziegler, J.P. Biersack, SRIM2000: The Stopping and Range of Ions in Matter, 2000, http://www.research.ibm.com/ionbeams/.
[11] P.E. Dodd, IEEE Trans. Nucl. Sci. NS 43 (1996) 561.